

# Analysis of Power System Dynamics Subject to Stochastic Power Injections

Sairaj V. Dhople, *Member, IEEE*, Yu C. Chen, *Student Member, IEEE*, Lee DeVille, and Alejandro D. Domínguez-García, *Member, IEEE*

**Abstract**—We propose a framework to study the impact of stochastic active/reactive power injections on power system dynamics with a focus on time scales involving electromechanical phenomena. In this framework the active/reactive power injections evolve according to a continuous-time Markov chain (CTMC), while the power system dynamics are described by the standard differential algebraic equation (DAE) model. The DAE model is linearized around a nominal set of active/reactive power injections; and the combination of the linearized DAE model and the CTMC forms a stochastic process known as a Stochastic Hybrid System (SHS). The extended generator of the SHS yields a system of ordinary differential equations that governs the evolution of the power system dynamic and algebraic state moments. We illustrate the application of the framework to the computation of long-term power system state statistics; and to short-term probabilistic dynamic performance/reliability assessment.

**Index Terms**—Continuous time Markov chains, Power system dynamics, Stochastic Hybrid Systems.

## I. INTRODUCTION

Power system operating conditions are facing increased uncertainty due to the integration of renewable resources such as wind energy conversion systems (WECS) and photovoltaic energy conversion systems (PVECS), and loads such as plug-in hybrid electric vehicles [1]. This uncertainty affects the system across different time scales—from day-ahead scheduling to automatic generation control and governor response [2]. In this paper, we focus on the impact of this uncertainty on power system dynamic performance at time scales involving electromechanical phenomena. Within this context, the system sees the effect of this uncertainty as a stochastic power injection and the problem is to compute the statistics of the system dynamic states, e.g., synchronous machines angles and speeds, and algebraic states, e.g., bus-voltage magnitudes and angles (in the remainder, we use the term *power injection* to refer to both power generation sources and loads). To address this problem, we propose an analytical framework that builds

on a set of tools developed for a class of stochastic processes referred to as Stochastic Hybrid Systems (SHS) [3].

In our framework, the power system dynamics are described by the standard nonlinear differential algebraic (DAE) model [4]; however, the active/reactive power injections in certain buses of the network are uncertain and their evolution is described by a continuous-time Markov chain (CTMC). [Below, we will describe a wide class of power generation resources and loads that can be described by such a model.] Transitions between states of the CTMC correspond to changes in active/reactive power injections. Since these changes are stochastic, the evolution of the dynamic and algebraic states (as described by the DAE) is also stochastic. In general, it is not possible to analytically obtain the joint probability density function (pdf) of the dynamic/algebraic states; furthermore, attempting to numerically obtain the pdf is computationally expensive. Thus, given the difficulty in obtaining the pdfs, we propose an analytical method to compute the moments of the power system dynamic and algebraic states. The moments can then be used, e.g., to compute bounds on the distribution or bounds on probabilities of different events of interest. Then, in the context we consider here, one only needs to compute as many moments as one needs to know for a particular application, and this is in general much less information than one would need to completely determine the pdf.

The proposed method casts the combination of the (linearized) power system dynamic model and the CTMC-based active/reactive power injection model as an SHS. The state space of an SHS is comprised of: i) a discrete state that, in the context of this paper, describes the possible values that the active/reactive power injections take; and ii) a continuous state that, in the context of this paper, describes the power system dynamic states, e.g., synchronous machine angles and speeds. The discrete state evolves according to a CTMC, and takes values in a finite set—the elements of which we will refer to as modes (each mode corresponds to a different combination of active/reactive power injections). The nonlinear DAE model is linearized around a nominal set of active/reactive power injections; the input to this linearized system is a vector comprised of the mode-dependent active/reactive power injections. In addition to the standard SHS formulation that includes the processes that describe how discrete and continuous states evolve, we introduce a third process that describes the evolution of the power system algebraic states, i.e., bus-voltage magnitudes and angles. Then, we formulate the SHS extended generator, and using Dynkin’s formula, obtain the moments of the dynamic and algebraic states [3]. It is worth noting

S. V. Dhople is with the Department of Electrical and Computer Engineering of the University of Minnesota, e-mail: {sdhople@UMN.EDU}.

Y. C. Chen and A. D. Domínguez-García are with the Department of Electrical and Computer Engineering of the University of Illinois at Urbana-Champaign, and L. DeVille is with the Department of Mathematics of the University of Illinois at Urbana-Champaign. e-mail: {chen267, aledan, rdeville}@ILLINOIS.EDU.

This work was supported in part by the National Science Foundation (NSF) under grant ECCS-CAR-0954420.

Copyright ©2013 IEEE. Personal use of this material is permitted. However, permission to use this material for any other purposes must be obtained from the IEEE by sending an email to pubs-permissions@ieee.org.

that our approach to quantify the impact of uncertainty in a nonlinear DAE system by linearizing it, and casting the resulting affine dynamic system within the SHS framework, may have applicability beyond the power system domain to other application areas where SHS are utilized.

The assumptions that we make are not restrictive; indeed, linear models are widely used to study the impact of small-signal disturbances on power-system dynamics [5], [6]. Similarly, as described next, a variety of stochastic loads and power sources can be modeled as CTMCs. Regarding uncertain loads, the Markovian assumption adopted in this work is consistent with well-established power-system load models (see, e.g., [7]–[11] and the references therein). Earlier works have also used SHS-like modeling formalisms to describe aggregate models of thermostatically controlled heating/cooling loads [12]–[15]. In these models, the dynamic states might represent the temperature of a building, while the discrete state might represent the operating state of the heating/cooling device. Regarding uncertain sources, an important application of the proposed framework is to evaluate the impact of renewable-based generation on power system dynamics. With respect to this, inputs to renewable energy systems (e.g., wind speeds in WECS, and incident solar insolation in PVECS) are inherently uncertain, and it is common to use Markov models to describe them (see, e.g., [16], [17] for wind speed models, and [18], [19] for solar insolation models). These models can then be combined with standard WECS and PVECS performance models that describe their power output (see, e.g., [20]–[23]). The load models and renewable-based power generation models described above can be incorporated within our framework straightforwardly through state-space augmentation. For uncertain loads, transition rates can be determined from appropriately defined load levels given historical load curves using the so-called multilevel load representation method [7, pp. 128–131]. With regard to renewable resources, the transition rates can be computed from the number of transitions between different states (each state corresponds to a range of wind speeds or a range of irradiance levels) over the period of observation [16]–[19].

The SHS-based framework proposed here integrates two disjoint bodies of work; namely the literature in hybrid-system approaches to power system performance assessment (see, e.g., [24]–[28] and the references therein), and the stochastic transient stability assessment literature (see, e.g., [29]–[36] and the references therein). In particular, our methodology is closely related to [29], which established a framework for probabilistic steady-state and dynamic security assessment of power systems (see also [37], [38] for related work). The authors in [29] consider different modes among which the power system can transition in a stochastic fashion, and derive a linear differential equation whose solution yields the distribution of a performance metric—this is done from first principles, and SHS tools are not employed. In [39]–[41], decentralized control methods for stabilization of power systems are presented where uncertainties are modeled using a Markov jump linear systems framework. It is worth noting that the models in [29], [39], [40] can all be described with SHS formalisms; in particular, it is easy to show that Markov

jump linear systems are a type of SHS.

The remainder of this paper is organized as follows. In Section II, we develop the stochastic model that describes the electromechanical behavior of a power system. In Section III, we describe an approach to obtain the moments of the dynamic and algebraic power-system states. Finally, in order to illustrate the ideas presented in Sections II and III, three numerical case studies involving 3-, 9- and 145-bus test systems are presented in Section IV. Concluding remarks and avenues for future work are summarized in Section V.

## II. STOCHASTIC POWER SYSTEM DYNAMIC MODEL

In this section, we first derive the linearized power system dynamic model that explicitly captures active/reactive power injections as inputs. We then combine this linearized model with the CTMC-based stochastic power injection model to obtain a stochastic model that describes the power system electromechanical behavior.

### A. Linearized Power System Dynamic Model

The power system electromechanical behavior can be described by a differential algebraic equation (DAE) model:

$$\dot{x} = f(x, y), \quad 0 = g(x, y, u), \quad (1)$$

where  $x(t) \in \mathbb{R}^n$  is referred to as the *dynamic state* (it includes the synchronous machine angles and speeds);  $y(t) \in \mathbb{R}^p$  is referred to as the *algebraic state* (it includes the bus-voltage magnitudes and angles);  $u(t) = [P_1(t), Q_1(t), \dots, P_r(t), Q_r(t)]^T \in \mathbb{R}^{2r}$ , where  $P_i(t)$  and  $Q_i(t)$  are the (possibly) uncertain active and reactive power injections in bus  $i$ , respectively;  $f: \mathbb{R}^{n+p} \rightarrow \mathbb{R}^n$  describes the evolution of the dynamic states, and  $g: \mathbb{R}^{n+p+2r} \rightarrow \mathbb{R}^p$  describes the power flow equations.

Let  $(x^*, y^*)$  denote some stable equilibrium point of (1) that results from some nominal active/reactive power injection profile given by  $u^* = [P_1^*, Q_1^*, \dots, P_r^*, Q_r^*]^T$ . Assume that  $f(\cdot, \cdot)$  and  $g(\cdot, \cdot, \cdot)$  in (1) are continuously differentiable and the power-flow Jacobian evaluated at  $(x^*, y^*, u^*)$ , i.e.,  $\partial g / \partial y|_{(x^*, y^*, u^*)}$ , is non-singular. Then, by linearizing (1) around  $(x^*, y^*, u^*)$ , we can obtain a linear model that approximates the evolution of  $x(t)$  and  $y(t)$  as follows:

$$\begin{aligned} \dot{x} &= Ax + Bu + C, \\ y &= Dx + Eu + F, \end{aligned} \quad (2)$$

where the entries of the matrices  $A, \dots, F$  are obtained from the Jacobians of  $f(\cdot, \cdot)$  and  $g(\cdot, \cdot, \cdot)$  evaluated at  $(x^*, y^*, u^*)$ . The complete derivation of (2), including the exact expressions for  $A, \dots, F$ , is provided in Appendix A.

### B. Power System Dynamics Stochastic Model

In order to completely characterize the power system dynamic model in (2), we need to define the stochastic model that describes the evolution of the (uncertain) active/reactive power injection vector  $u(t)$ . To this end, beyond the nominal value  $u^*$  of the active/reactive power injection vector that we used for obtaining (2), we assume that: i) at each time instant  $t$ ,  $u(t)$  can

additionally take  $N$  different values, each of which is denoted by  $u^i = [P_1^i, Q_1^i, \dots, P_r^i, Q_r^i]^\top \in \mathbb{R}^{2r}, i = 0, \dots, N$  (as a matter of convention, we establish  $u^0 = u^*$ ); and ii) the evolution of  $u(t)$  is governed by a discrete-state continuous-time stochastic process  $Q(t)$  taking values in  $\mathcal{Q} = \{0, 1, \dots, N\}$ ; specifically, whenever  $Q(t) = i$ , then  $u(t) = u^i$ . In subsequent developments, we will refer to the elements of  $\mathcal{Q}$  as *modes*.

**Remark 1.** The affine model in (2) was obtained by linearizing (1) around the equilibrium point that results from  $u = u^*$ ; thus, the equilibrium point of (2) coincides with the equilibrium point of (1) whenever  $u = u^*$ . We assume that the change in  $u$  around  $u^*$  is small enough so that the linearization is accurate and, for  $u \neq u^*$ , the location of the equilibrium point in (2) is close to the corresponding one in (1). For example, this linearization was shown to be accurate in [6] for a 54-state system, and variations in the entries of  $u$  up to 50% around their nominal values. Following [26], a different approach would consist of linearizing (1) around the equilibrium point that results from each  $u^i, i \in \mathcal{Q}$ ; this would result in a collection of affine systems instead of the single one in (2). More importantly, as highlighted in [26], this approach would also enable the modeling of system topology changes induced by faults, e.g., transmission line tripping events or generator outages.  $\square$

In light of the above discussion, it is important to note that since  $Q(t)$  governs the evolution of the (uncertain) active/reactive power injections, we can define a stochastic process  $U(Q(t))$  that describes the values that  $u(t)$  in (2) can take. The power system dynamic and algebraic states  $x(t)$  and  $y(t)$  (the evolution of which is described by (2)), are now continuous-state continuous-time stochastic processes, which we denote by  $X(t)$  and  $Y(t)$ , respectively. Next, we provide a formal description of the stochastic process that results from combining  $Q(t)$ ,  $X(t)$ , and  $Y(t)$ .

Let  $\mathcal{Q}_i^+ \subseteq \mathcal{Q}$  denote the set of all modes that  $Q(t)$  can transition to, given that  $Q(t) = i$ ; we can then define two functions

$$\lambda_{ij}: \mathcal{Q} \times \mathbb{R}^n \times \mathbb{R}^+ \rightarrow \mathbb{R}^+, \quad (3)$$

$$\phi_{ij}: \mathcal{Q} \times \mathbb{R}^n \times \mathbb{R}^+ \rightarrow \mathcal{Q} \times \mathbb{R}^n, \quad (4)$$

that govern the transitions amongst the modes. The  $\lambda_{ij}$ 's are the *transition rates* that govern the times when the system switches from mode  $i$  to mode  $j$ , and the  $\phi_{ij}$ 's are the *transition reset maps* that tell us how the states change after a transition.

More specifically, we impose on the system that, given it is in mode  $i$  at time  $t$ , i.e.,  $\Pr\{Q(t) = i\} = 1$ , then the probability that the discrete state transitions to mode  $j$  in the time interval  $[t, t + \tau)$  is given by

$$\lambda_{ij}(Q(t), X(t), t)\tau + o(\tau) = \lambda_{ij}(i, X(t), t)\tau + o(\tau), \quad (5)$$

and the probability of a transition out of mode  $i$  is given by

$$\sum_{j \in \mathcal{Q}_i^+} \lambda_{ij}(Q(t), X(t), t)\tau + o(\tau). \quad (6)$$

If the  $i \rightarrow j$  transition occurs, the new values of  $Q$  and  $X$  are

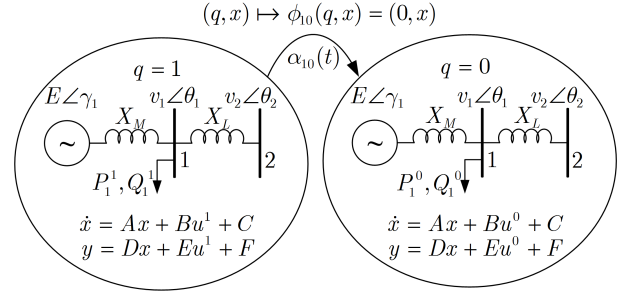


Figure 1. Two-mode stochastic model for the SMIB system of Example 1.

defined<sup>1</sup> to be

$$(Q(t + \tau), X(t + \tau)) = \phi_{ij}(Q((t + \tau)^-), X((t + \tau)^-), t + \tau). \quad (7)$$

The probability that no transition out of state  $i$  occurs in the time interval  $[t, t + \tau)$  is given by

$$1 - \tau \sum_{k \in \mathcal{Q}_i^+} \lambda_{ik}(i, X(t), t), \quad (8)$$

and until a transition occurs, the evolution of the dynamic and algebraic state is determined by setting  $u(t) = u^i$  in (2). Thus, the evolution of  $X(t)$  and  $Y(t)$  can be described by

$$\begin{aligned} dX(t) &= (A X(t) + B U(Q(t)) + C) dt, \\ Y(t) &= D X(t) + E U(Q(t)) + F. \end{aligned} \quad (9)$$

**Remark 2.** The definition of the transitions is slightly overloaded; for instance,  $\lambda_{ij}$  should be positive only if  $Q(t) = i$ , since the probability of the system making an  $i \rightarrow j$  transition when  $Q(t)$  is not equal to  $i$  is zero. Thus we do not need  $\lambda_{ij}, \phi_{ij}$  to depend on  $q$ ; however, we impose throughout<sup>2</sup> that

$$\lambda_{ij}(q, x, t) = \delta_i(q) \alpha_{ij}(x, t). \quad (10)$$

This seems like an unnecessary layer of complexity at this point; however, we will see below that this notation significantly simplifies the calculations.  $\square$

While it is certainly possible in the general SHS framework for the maps  $\phi_{ij}$  to change both  $Q(t)$  and  $X(t)$  at the time of the jump, in this work, we assume throughout that

$$\phi_{ij}(q, x) = (j, x). \quad (11)$$

This means that  $X(t)$  does not undergo an instantaneous jump at the moment of transition since power system dynamic states do not change instantaneously with step changes in active/reactive power injections [24].

Next, we illustrate the notation introduced so far with a simple example.

**Example 1.** Figure 1 depicts a Single-Machine Infinite-Bus (SMIB) system comprised of a synchronous generator connected to bus 1 and a load connected to bus 2. Let  $\gamma_1$  and

<sup>1</sup>The left-hand limit of the function  $f(t)$  is denoted by  $f(t^-)$ , i.e.,  $f(t^-) := \lim_{s \nearrow t} f(s)$ .

<sup>2</sup>We use the Kronecker delta function notation:  $\delta_i(q) = 1$  if  $i = q$  and  $\delta_i(q) = 0$  if  $i \neq q$ .

$\omega_1$  denote the synchronous generator rotor angular position and velocity, respectively. Let  $v_1$  and  $v_2$  denote the voltage magnitudes of buses 1 and 2, respectively, and let  $\theta_1$  and  $\theta_2$  denote voltage angles of buses 1 and 2, respectively. Then the system DAE model (assuming that the synchronous generator is described by the classical model) is given by

$$\begin{aligned}\dot{\gamma}_1 &= \omega_1 - \omega_s, \\ \dot{\omega}_1 &= \frac{1}{M} \left( P_M - \frac{Ev_1}{X_L} \sin(\gamma_1 - \theta_1) - D(\omega_1 - \omega_s) \right), \\ 0 &= \frac{Ev_1}{X_M} \sin(\gamma_1 - \theta_1) - \frac{v_1 v_2}{X_L} \sin(\theta_1) - P_1, \\ 0 &= \frac{Ev_1}{X_M} \cos(\theta_1 - \gamma_1) - \frac{v_1^2}{X_M} \\ &\quad + \frac{v_1 v_2}{X_L} \cos(\theta_1) - \frac{v_1^2}{X_L} - Q_1,\end{aligned}\quad (12)$$

where  $P_1$ ,  $Q_1$  are the power injections at bus 1,  $\omega_s$  is the synchronous speed (377 rad/s),  $M$  is the machine inertia constant,  $X_M$  is the synchronous generator reactance,  $D$  is the damping coefficient,  $E$  is the generator internal voltage, and  $X_L$  is the reactance of the line connecting buses 1 and 2.

Suppose the nominal active/reactive power injections at bus 1 are given by  $u^0 = u^* = [P_1^0, Q_1^0]^T = [P_1^*, Q_1^*]^T$ . The corresponding equilibrium values of the system states are denoted by  $\gamma_1^*$ ,  $\omega_1^*$ ,  $v_1^*$ , and  $\theta_1^*$ . Linearizing (12) around this equilibrium point, we get an affine system of the form in (2). Now, consider the case when the active/reactive power injections are given by  $u^1 = [P_1^1, Q_1^1]^T$ . The duration for which the power injections are not the nominal values, is uncertain and can be described by a random variable  $T$ , with pdf and cdf denoted by  $f_T(t)$  and  $F_T(t)$ , respectively. Then, following the notation introduced earlier,  $Q(t)$  takes values in  $\mathcal{Q} = \{0, 1\}$  and there is a single transition from mode 1 to 0; this implies that  $\mathcal{Q}_0^+ = \{1\}$ , and  $\mathcal{Q}_1^+ = \emptyset$ . The transition rate is given by the hazard rate of the distribution of  $T$ , i.e.,  $\lambda_{10}(q, t) = \delta_1(q)(f_T(t)/(1 - F_T(t))) =: \delta_1(q)\alpha_{10}(t)$ . Since  $\gamma_1$  and  $\omega_1$  do not jump due to the transition, the reset map is given by  $\phi_{10}(q, x) = (0, x)$ . ■

In large power systems, the uncertain power injections might take a very large number of values, resulting in a very large number of discrete states. To address the computational challenges associated with tackling a large number of states, model-reduction methods have been proposed for Markov chains and jump-linear systems, which are a subset of the more general SHS we study in this work (see, e.g., [42]–[45]); similar techniques may be applied to the SHS framework examined in this paper.

Instead of dedicating a mode to describe every value that the uncertain power injections can take, the variability in the power injections can be captured by expressing  $u$  as a continuous-time stochastic process; the evolution of  $u$  is then described by a stochastic differential equation (SDE). This approach is outlined in Appendix B.

### III. POWER SYSTEM DYNAMICS STOCHASTIC ANALYSIS

The stochastic process in (9) that results from combining the stochastic power injection model (governed by  $Q(t)$ ) and

the linearized power system dynamic model (as described in (2)) belongs to a class of stochastic processes known as stochastic hybrid systems (SHS) [3]. In the most general SHS, the evolution of  $X(t)$  (in between transitions of  $Q(t)$ ) is governed by a nonlinear SDE. Additionally, the reset maps can also induce jumps in  $X(t)$ . In (7) we define the reset maps  $\phi_{ij}$  so that only  $Q(t)$  changes once a transition occurs.

For the special case when the SDEs describing the flow of  $X(t)$ , the reset maps, and transition rates, are polynomial functions of  $X(t)$ , analytical methods have been proposed in [3], [46] to obtain the evolution of the moments of  $Q(t)$  and  $X(t)$ . The moments in these systems are governed by an infinite-dimensional system of ODEs, simply due to the fact that the evolution of the  $p^{\text{th}}$  moment depends, in general, on moments higher than  $p$ . In this sense, any finite approximation to the actual system will be a differential equation containing terms on the right-hand side that do not appear on the left-hand side, and thus the equations are not *closed*. Consequently, methods to truncate the ODEs have to be applied for analysis and simulation. These methods are commonly referred to as *moment-closure methods* (see, e.g., [3], [47]).

However, we will show that for the power system SHS model considered in this paper, the system of ODEs we obtain when we seek to track any finite number of moments of  $Q(t)$  and  $X(t)$  is finite-dimensional. Thus moment-closure methods are made unnecessary. Towards this end, we first define the extended generator of the power system SHS model, and then following along [3], describe a general method to formulate appropriate test functions that yield the moments of interest by applying Dynkin's formula.

#### A. Extended Generator of the Power Systems SHS Model

Consider the power systems SHS model described in Section II-B. Let  $\psi: \mathcal{Q} \times \mathbb{R}^n \rightarrow \mathbb{R}$  be any function (we will refer below to this as a *test function*). We will also write this as  $\psi(q, x)$ , where  $q$  denotes the mode, and  $x$  denotes the power system dynamic state.

The *generator of the SHS* is the linear operator defined by:

$$\begin{aligned}(L\psi)(q, x) &= \frac{\partial}{\partial x} \psi(q, x) \cdot (Ax + Bu^q + C) \\ &\quad + \sum_{i,j \in \mathcal{Q}} \lambda_{ij}(q, x) \left( \psi(\phi_{ij}(q, x)) - \psi(q, x) \right).\end{aligned}\quad (13)$$

where  $\partial\psi/\partial x \in \mathbb{R}^{1 \times n}$  denotes the gradient of  $\psi(q, x)$  with respect to  $x$ , and  $\lambda_{ij}(q, t)$  is the transition rate for the  $i \rightarrow j$  transition. The definition of the generator above follows from [3], [46], [48].

The evolution of the expected value of the test function  $\mathbb{E}[\psi(Q(t), X(t))]$ , is governed by Dynkin's formula, which can be stated in differential form as follows [46], [48]:

$$\frac{d}{dt} \mathbb{E}[\psi(Q(t), X(t))] = \mathbb{E}[(L\psi)(Q(t), X(t))].\quad (14)$$

Said in words, (14) indicates that the rate of change of the expected value of a test function evaluated on the stochastic process is given by the expected value of the generator. This makes intuitive sense: the first line in (13) captures the total derivative of the test function with respect to time,

and the second line captures the impact of incoming/outgoing transitions [3], [47].

To derive this operator, one proceeds as follows. Let us first define the operator  $L$  on the space  $C^1 \cap L^\infty$  (i.e., all bounded and continuously-differentiable functions) to be the one that satisfies (14). One can compute by hand that it must have the formula in (13). Of course, the problem here is that the generator has a differential piece, but we might want to apply it to functions that are not differentiable (e.g., indicator functions). One then extends the definition of  $L$  as follows: given a specific target function  $f$ , if we can construct a sequence of functions  $\{f_n\}_{n=1}^\infty$  such that  $\lim_{n \rightarrow \infty} f_n = f$ , then we define  $Lf = \lim_{n \rightarrow \infty} Lf_n$ . It can be shown that this definition produces a computable and consistent result for all functions in a particular set  $\mathcal{B}$ , which we do not explicitly describe, but which we point out contains all indicator functions (functions of the form  $1_A(x)$  for some Borel set  $A$ ) and monomials ( $x^p$  for some power  $p$ ). The specific details of this construction, and a definition of the set  $\mathcal{B}$ , is contained in [48].

We will show that by a judicious choice of test functions, we can use (14) to obtain ODEs that describe the evolution of relevant conditional moments of interest. From this, the law of total expectation will yield the desired moments of the dynamic/algebraic states; we describe this procedure next.

### B. Test Functions for the Power Systems SHS Model

For the power system SHS model where the discrete state  $Q(t)$  takes values in the set  $\mathcal{Q}$ , we define the following family of test functions:

$$\psi_i^{(m)}(q, x) := \delta_i(q)x^m = \begin{cases} x^m & \text{if } q = i \\ 0 & \text{if } q \neq i \end{cases}, \forall i \in \mathcal{Q}, \quad (15)$$

where  $m := (m_1, m_2, \dots, m_n) \in \mathbb{N}^{1 \times n}$ , and  $x^m := x_1^{m_1} x_2^{m_2} \dots x_n^{m_n}$ . We will show later that the definition of the test functions with the aid of Kronecker delta functions greatly eases the derivation of the ODEs governing the moments of  $X(t)$  and  $Y(t)$ . We also define the conditional moments of the dynamic state  $X(t)$  at time  $t$ ,  $\mu_i^{(m)}(t)$ ,  $\forall i \in \mathcal{Q}$ , as follows:

$$\mu_i^{(m)}(t) := \mathbb{E}[\psi_i^{(m)}(q, x)] = \mathbb{E}[X^{(m)}(t)|Q(t) = i] \pi_i(t), \quad (16)$$

where  $\pi_i(t)$  denotes the occupational probability of mode  $i$ , i.e.,  $\pi_i(t) := \Pr\{Q(t) = i\}$ . The second equality above follows straightforwardly from the definition of the test functions.

For the algebraic state, we will not need dedicated test functions, because the conditional moments of the algebraic state can be directly expressed as a linear function of the conditional moments of the dynamic state. Therefore, our strategy will be to use Dynkin's formula to obtain ODEs that govern the evolution of the  $\mu_i^{(m)}$ 's, and then use the algebraic relation in (9) to obtain the conditional moments of the algebraic state directly. Towards this end, define the conditional moments of the algebraic state  $Y(t)$  at time  $t$ ,  $\zeta_i^{(m)}(t)$ ,  $\forall i \in \mathcal{Q}$ , as follows:

$$\zeta_i^{(m)}(t) := \mathbb{E}[Y^{(m)}(t)|Q(t) = i] \pi_i(t). \quad (17)$$

By appropriately picking the  $m_i$ 's in (16)-(17), we can isolate any conditional moment of interest; we demonstrate this in

the context of the SMIB SHS model introduced earlier in Example 1.

**Example 2.** Recall the SMIB system described in Example 1. Associated with the two modes  $i = \{0, 1\}$ , define the test functions  $\psi_i^{(m)}(q, x) = \delta_i(q)x^m$ , where  $m = (m_1, m_2) \in \mathbb{N}^{1 \times 2}$  and  $x^m = \gamma_1^{m_1} \omega_1^{m_2}$ . Also, denote the conditional moments of the dynamic and algebraic states by  $\mu_i^{(m)}(t)$  and  $\zeta_i^{(m)}(t)$ , respectively. By appropriately picking  $m$  in (16)–(17), we can recover many conditional moments of interest. For instance, note that choosing  $m = (0, 0)$  recovers the occupational probabilities of the modes,

$$\mu_i^{(0,0)}(t) = \zeta_i^{(0,0)}(t) = \Pr\{Q(t) = i\} = \pi_i(t). \quad (18)$$

Similarly, picking  $m = (2, 0)$  isolates the second-order conditional moment of  $\Gamma(t)$  and  $V_1(t)$

$$\begin{aligned} \mu_i^{(2,0)}(t) &= \mathbb{E}[X^{(2,0)}(t)|Q(t) = i] \cdot \pi_i(t) \\ &= \mathbb{E}[\Gamma_1^2(t)|Q(t) = i] \cdot \pi_i(t), \end{aligned} \quad (19)$$

$$\begin{aligned} \zeta_i^{(2,0)}(t) &= \mathbb{E}[Y^{(2,0)}(t)|Q(t) = i] \cdot \pi_i(t) \\ &= \mathbb{E}[V_1^2(t)|Q(t) = i] \cdot \pi_i(t). \end{aligned} \quad (20)$$

Finally, picking  $m = (1, 1)$  yields the conditional expectation of the product  $\Gamma(t) \cdot \Omega(t)$  and  $V_1(t) \cdot \Theta_1(t)$

$$\begin{aligned} \mu_i^{(1,1)}(t) &= \mathbb{E}[X^{(1,1)}(t)|Q(t) = i] \cdot \pi_i(t) \\ &= \mathbb{E}[\Gamma_1(t)\Omega_1(t)|Q(t) = i] \cdot \pi_i(t), \end{aligned} \quad (21)$$

$$\begin{aligned} \zeta_i^{(1,1)}(t) &= \mathbb{E}[Y^{(1,1)}(t)|Q(t) = i] \cdot \pi_i(t) \\ &= \mathbb{E}[V_1(t)\Theta_1(t)|Q(t) = i] \cdot \pi_i(t). \end{aligned} \quad (22)$$

Following a similar procedure to the one outlined above, we can recover any desired moment of interest with an appropriate choice of  $m$ . ■

### C. Evolution of the Dynamic- and Algebraic-State Moments

Now that we have outlined how different conditional moments can be defined, we explain how the law of total expectation is applied to obtain the moments of  $X(t)$  and  $Y(t)$  from these conditional moments. We then derive ODEs that govern the evolution of the conditional moments of  $X(t)$ , and explain how the algebraic relationship in (9) yields the moments of  $Y(t)$ . The analysis below follows from the methods developed in [3], [48].

Suppose we want to compute  $\mathbb{E}[X^m(t)]$ ,  $\mathbb{E}[Y^m(t)]$  for some  $m \in \mathbb{N}^{1 \times n}$ . Applying the law of total expectation, we see that these are given by

$$\begin{aligned} \mathbb{E}[X^m(t)] &= \sum_{i \in \mathcal{Q}} \mathbb{E}[X^m(t)|Q(t) = i] \pi_i(t) = \sum_{i \in \mathcal{Q}} \mu_i^{(m)}(t), \\ \mathbb{E}[Y^m(t)] &= \sum_{i \in \mathcal{Q}} \mathbb{E}[Y^m(t)|Q(t) = i] \pi_i(t) = \sum_{i \in \mathcal{Q}} \zeta_i^{(m)}(t). \end{aligned} \quad (23)$$

Therefore, at each time  $t$ , to obtain  $\mathbb{E}[X^m(t)]$ , we need to know the conditional moments of  $X(t)$ ,  $\mu_i^{(m)}(t)$ ,  $\forall i \in \mathcal{Q}$ ; and

to obtain  $\mathbb{E}[Y^m t]$ , we need to know the conditional moments of  $Y(t)$ ,  $\zeta_i^{(m)}(t)$ ,  $\forall i \in \mathcal{Q}$ . The SHS framework—particularly Dynkin’s formula as prescribed in (14)—yields ODEs that govern the evolution of  $\mu_i^{(m)}(t)$ . Since the relationship between  $X(t)$  and  $Y(t)$  is purely algebraic, the  $\zeta_i^{(m)}$ ’s can be obtained from the  $\mu_i^{(m)}$ ’s in a straightforward manner. Next, we derive the ODE’s that govern the evolution of the  $\mu_i$ ’s, and describe how the  $\zeta_i$ ’s can be obtained using (9) and the  $\mu_i$ ’s.

1) *Evolution of the Dynamic-State Conditional Moments:*

The evolution of  $\mu_i^{(m)}(t)$ ,  $\forall i \in \mathcal{Q}$ , is governed by Dynkin’s formula

$$\dot{\mu}_i^{(m)}(t) = \frac{d}{dt} \mathbb{E}[\psi_i^{(m)}(q, x)] = \mathbb{E}[(L\psi_i^{(m)})(q, x)]. \quad (24)$$

Given the power-system SHS model in (9) and the test functions in (15), it turns out that  $\mathbb{E}[(L\psi_i^{(m)})(q, x)]$  can be significantly simplified and expressed as a function of the  $\mu_i$ ’s to recover a closed set of ODEs. Towards this end, substituting the extended generator from (13) in Dynkin’s formula above, and using the linearity of the expectation operator, we obtain the following relation:

$$\begin{aligned} \dot{\mu}_i^{(m)}(t) &= \mathbb{E} \left[ (L\psi_i^{(m)})(q, x) \right] \\ &= \mathbb{E} \left[ \frac{\partial}{\partial x} \psi_i^{(m)} \cdot (Ax + Bu^i + C) \right] \\ &\quad + \mathbb{E} \left[ \sum_{j \in \mathcal{Q}_i^-} \lambda_{ji}(q, t) \psi_i^{(m)}(\phi_{ji}(q, x)) \right] \\ &\quad - \mathbb{E} \left[ \sum_{k \in \mathcal{Q}_i^+} \lambda_{ik}(q, t) \psi_i^{(m)}(q, x) \right], \end{aligned} \quad (25)$$

where  $\mathcal{Q}_i^- \subseteq \mathcal{Q}$  is the set of all modes from which  $Q(t)$  can transition to mode  $i$ , and  $\mathcal{Q}_i^+ \subseteq \mathcal{Q}$  is the set of all modes that  $Q(t)$  can transition into from mode  $i$ . Now consider the second line in (25). We will simplify the two terms in the dot product  $(\partial\psi_i/\partial x) \cdot (Ax + Bu^i + C)$  separately. First, from the definition of the test function in (15) we obtain

$$\begin{aligned} \frac{\partial}{\partial x} \psi_i^{(m)}(q, x) &= \delta_i(q) \begin{bmatrix} m_1 x^{(m_1-1, m_2, \dots, m_n)} \\ \vdots \\ m_n x^{(m_1, m_2, \dots, m_{n-1})} \end{bmatrix}^T \\ &= \delta_i(q) \begin{bmatrix} m_1 x^{m-e_1} \\ \vdots \\ m_n x^{m-e_n} \end{bmatrix}^T, \end{aligned} \quad (26)$$

where  $e_i \in \mathbb{N}^{1 \times n}$  is the row vector with a 1 as the  $i$ th entry and zero otherwise. Next, to simplify terms in  $(Ax + Bu^i + C)$ , denote the entry in the  $p$ th row and  $q$ th column of the matrices  $A$  and  $B$  by  $a_{pq}$  and  $b_{pq}$ , respectively, and the  $p$ th element of the vectors  $C$  and  $Bu^i + C$  by  $c_p$  and  $v_p^i$ , respectively. We can then express the  $p$ th entry of the vector  $Ax + Bu^i + C$  as

$$\sum_{r=1}^n (a_{pr} \delta_i(q) x^{m-e_p+e_r} + \delta_i(q) x^{m-e_p} v_p^i). \quad (27)$$

Taking the dot product of (26) with the vector comprised of the entries given in (27), we get

$$\begin{aligned} &\frac{\partial}{\partial x} \psi_i^{(m)}(q, x) \cdot (Ax + Bu^i + C) \\ &= \sum_{k=1}^n m_k \left( \sum_{r=1}^n a_{kr} \delta_i(q) x^{m-e_k+e_r} + \delta_i(q) x^{m-e_k} v_k^i \right) \\ &= \sum_{k=1}^n m_k \left( \sum_{r=1}^n a_{kr} \psi_i^{(m-e_k+e_r)}(q, x) + v_k^i \psi_i^{(m-e_k)}(q, x) \right). \end{aligned} \quad (28)$$

The second equality above follows from the definition of the test functions, i.e.,  $\psi_i^{(m)}(q, x) = \delta_i(q) x^m$ . We go through some effort to express the above equation in terms of the  $\psi_i$ ’s, as this will be useful when deriving the differential equations that govern the conditional moments. Substituting (28) and the transition rates from (10) into (25), and recognizing that  $\phi_{ji}(q, x) = (i, x)$ , we obtain

$$\begin{aligned} \dot{\mu}_i^{(m)}(t) &= \\ &\mathbb{E} \left[ \sum_{p=1}^n m_p \left( \sum_{r=1}^n a_{pr} \psi_i^{(m-e_p+e_r)}(q, x) + v_p^i \psi_i^{(m-e_p)}(q, x) \right) \right] + \\ &\mathbb{E} \left[ \sum_{j \in \mathcal{Q}_i^-} \delta_j(q) \alpha_{ji}(t) \psi_i^{(m)}(i, x) - \sum_{k \in \mathcal{Q}_i^+} \delta_i(q) \alpha_{ik}(t) \psi_i^{(m)}(q, x) \right]. \end{aligned} \quad (29)$$

From the definition of the test functions, we see that  $\delta_j(q) \psi_i^{(m)}(i, x) = \delta_j(q) x^m$ , and  $\delta_i(q) \psi_i^{(m)}(q, x) = \delta_i(q) x^m$ . This allows us to simplify (29) as follows

$$\begin{aligned} \dot{\mu}_i^{(m)}(t) &= \\ &\mathbb{E} \left[ \sum_{p=1}^n m_p \left( \sum_{r=1}^n a_{pr} \psi_i^{(m-e_p+e_r)}(q, x) + v_p^i \psi_i^{(m-e_p)}(q, x) \right) \right] \\ &\quad + \sum_{j \in \mathcal{Q}_i^-} \alpha_{ji}(t) \mathbb{E}[\delta_j(q) x^m] - \sum_{k \in \mathcal{Q}_i^+} \alpha_{ik}(t) \mathbb{E}[\delta_i(q) x^m] \\ &= \sum_{p=1}^n m_p \left( \sum_{r=1}^n a_{pr} \mathbb{E}[\psi_i^{(m-e_p+e_r)}(q, x)] \right. \\ &\quad \left. + v_p^i \mathbb{E}[\psi_i^{(m-e_p)}(q, x)] \right) \\ &\quad + \sum_{j \in \mathcal{Q}_i^-} \alpha_{ji}(t) \mathbb{E}[\psi_j(q, x)] - \sum_{k \in \mathcal{Q}_i^+} \alpha_{ik}(t) \mathbb{E}[\psi_i(q, x)]. \end{aligned} \quad (30)$$

Finally, from the definition of the conditional moments in (16), we get the following set of ODEs

$$\begin{aligned} \dot{\mu}_i^{(m)}(t) &= \sum_{p=1}^n m_p \left( \sum_{r=1}^n a_{pr} \mu_i^{(m-e_p+e_r)}(t) + \mu_i^{(m-e_p)}(t) v_p^i \right) \\ &\quad + \sum_{j \in \mathcal{Q}_i^-} \alpha_{ji}(t) \mu_j^{(m)}(t) - \sum_{k \in \mathcal{Q}_i^+} \alpha_{ik}(t) \mu_i^{(m)}(t), \quad \forall i \in \mathcal{Q}. \end{aligned} \quad (31)$$

Note that the terms in the second line of (31) capture the impact of incoming and outgoing transitions (respectively) on  $\mu_i^{(m)}$ . Additionally, the derivation above indicates that the moment ODEs only depend on other conditional moments of

the same or lower order. In particular, this means that the ODEs in (31) are effectively finite-dimensional and moment-closure methods are unnecessary.

**Remark 3.** As discussed in the introduction, since the transition rates are not a function of the dynamic states, the discrete state is a CTMC. Therefore, using (31) we can recover the Chapman-Kolmogorov differential equations that govern the occupational probabilities of the CTMC. Towards this end, substitute  $m = (0, \dots, 0) \in \mathbb{R}^{1 \times n}$  in (31) to get

$$\dot{\mu}_i^{(0, \dots, 0)}(t) = \sum_{j \in \mathcal{Q}_i^-} \alpha_{ji}(t) \mu_j^{(0, \dots, 0)}(t) - \sum_{k \in \mathcal{Q}_i^+} \alpha_{ik}(t) \mu_i^{(0, \dots, 0)}(t). \quad (32)$$

From (18), we know that  $\mu_i^{(0, \dots, 0)}(t) = \pi_i(t) = \Pr\{Q(t) = i\}$ . Therefore, (32) can be expressed as

$$\dot{\pi}_i(t) = \sum_{j \in \mathcal{Q}_i^-} \alpha_{ji}(t) \pi_j(t) - \sum_{k \in \mathcal{Q}_i^+} \alpha_{ik}(t) \pi_i(t), \quad (33)$$

which are precisely the Chapman-Kolmogorov equations for the occupational probabilities of a CTMC [49].  $\square$

2) *Conditional Moments of the Algebraic States* : Once the conditional moments of  $X(t)$  (and the ODEs that govern their evolution) are in hand, we can use the algebraic relationship in (2) to obtain the conditional moments of  $Y(t)$  as follows:

$$\begin{aligned} \zeta_i^{(m)}(t) &= \mathbb{E}[Y^m(t) | Q(t) = i] \cdot \pi_i(t) \\ &= \mathbb{E}[(DX(t) + EU(i) + F)^m | Q(t) = i] \cdot \pi_i(t). \end{aligned} \quad (34)$$

While it is difficult to simplify (34) in symbolic form, it is clear that  $\zeta_i^{(m)}$  only depends on those  $\mu_i^{(k)}$  with  $|k|_{\ell^1} = |m|_{\ell^1}$  ( $|x|_{\ell^1}$  denotes the one-norm of vector  $x$ ), and the occupational probabilities.

Note that the approach outlined above provides a systematic method to obtain moments of the output,  $Y(t)$  (from a measurement equation of the form in (9)), given the statistics of the system state,  $X(t)$ , and input,  $U(Q(t))$ . Next, we demonstrate how (31) and (34) apply in practice with regard to the SMIB SHS model introduced earlier.

**Example 3.** Recall that in Example 2 we demonstrated how to obtain the conditional moments of interest in the SMIB model by picking  $m = (m_1, m_2) \in \mathbb{R}^{1 \times 2}$  appropriately. For a given choice of  $m$ , by applying (31), we get the following expressions for the ODEs that govern the conditional moments of the dynamic state:

$$\begin{aligned} \dot{\mu}_i^{(m)}(t) &= (m_1 a_{11} + m_2 a_{22}) \mu_i^{(m)}(t) \\ &+ m_1 a_{12} \mu_i^{(m_1-1, m_2+1)}(t) + m_2 a_{21} \mu_i^{(m_1+1, m_2-1)}(t) \\ &+ m_1 (b_{11} P_1^i + b_{12} Q_1^i + c_1) \mu_i^{(m_1-1, m_2)}(t) \\ &+ m_2 (b_{21} P_1^i + b_{22} Q_1^i + c_2) \mu_i^{(m_1, m_2-1)}(t) \\ &+ \delta_i(0) \left( \alpha_{10}(t) \mu_1^{(m)}(t) \right) + \delta_i(1) \left( -\alpha_{10}(t) \mu_1^{(m)}(t) \right). \end{aligned} \quad (35)$$

Suppose that we were interested in the evolution of  $\mathbb{E}[\Gamma_1(t)]$  and  $\mathbb{E}[\Omega_1(t)]$ , i.e., the first-order moments of the generator rotor position and angular velocity, respectively. To obtain  $\mathbb{E}[\Gamma_1(t)]$ , we would substitute  $m = (m_1, m_2) = (1, 0)$  in (31),

to get two ODEs (for  $i = 0, 1$ )

$$\begin{aligned} \dot{\mu}_i^{(1,0)}(t) &= a_{11} \mu_i^{(1,0)}(t) + a_{12} \mu_i^{(0,1)}(t) \\ &+ (b_{11} P_1^i + b_{12} Q_1^i + c_1) \mu_i^{(0,0)}(t) \\ &+ \delta_i(0) \left( \alpha_{10}(t) \mu_1^{(1,0)}(t) \right) + \delta_i(1) \left( -\alpha_{10}(t) \mu_1^{(1,0)}(t) \right). \end{aligned} \quad (36)$$

We would recover a similar set of ODEs for  $\mathbb{E}[\Omega_1(t)]$  by substituting  $m = (0, 1)$  in (31). To solve (36) (and the corresponding case for  $m = (0, 1)$ ), we would also need to concurrently solve ODEs for the occupational probabilities (i.e., the Chapman-Kolmogorov equations) which can be obtained from (33) as follows:

$$\begin{aligned} \dot{\mu}_1^{(0,0)}(t) &= \dot{\pi}_1(t) = -\alpha_{10}(t) \mu_1^{(0,0)}(t) = -\alpha_{10}(t) \pi_1(t), \\ \dot{\mu}_0^{(0,0)}(t) &= \dot{\pi}_0(t) = +\alpha_{10}(t) \mu_1^{(0,0)}(t) = +\alpha_{10}(t) \pi_1(t). \end{aligned} \quad (37)$$

In summary, we would simulate the system of ODEs  $(\dot{\mu}_0^{(0,0)}, \dot{\mu}_1^{(0,0)}, \dot{\mu}_0^{(1,0)}, \dot{\mu}_1^{(1,0)}, \dot{\mu}_0^{(0,1)}, \dot{\mu}_1^{(0,1)})$  and then apply  $\mathbb{E}[\Delta_1(t)] = \mu_0^{(1,0)}(t) + \mu_1^{(1,0)}(t)$  and  $\mathbb{E}[\Omega_1(t)] = \mu_0^{(0,1)}(t) + \mu_1^{(0,1)}(t)$  to obtain the moments of interest. Notice that the system of ODEs we need to solve is closed, in the sense that they do not involve second- or higher-order terms; therefore moment-closure methods are unnecessary.

The conditional moments of the algebraic states can be obtained from (34). Suppose we were interested in computing  $\mathbb{E}[V_1(t)]$  and  $\mathbb{E}[\Theta_1(t)]$ . We would first obtain the conditional moments  $\zeta_i^{(1,0)}(t)$  and  $\zeta_i^{(0,1)}(t)$  using (34) as follows:

$$\begin{aligned} \zeta_i^{(1,0)}(t) &= d_{11} \mu_i^{(1,0)}(t) + d_{12} \mu_i^{(0,1)}(t) \\ &+ (e_{11} P_1^i + e_{12} Q_1^i + f_1) \pi_i(t), \end{aligned} \quad (38)$$

$$\begin{aligned} \zeta_i^{(0,1)}(t) &= d_{21} \mu_i^{(1,0)}(t) + d_{22} \mu_i^{(0,1)}(t) \\ &+ (e_{21} P_1^i + e_{22} Q_1^i + f_2) \pi_i(t), \end{aligned} \quad (39)$$

where we denote the entry in the  $p$  row and  $q$  column of the matrices  $D$  and  $E$  by  $d_{pq}$  and  $e_{pq}$ , respectively, and the  $p$  element of the vectors  $f$  by  $f_p$ . Then, applying (23), we get  $\mathbb{E}[V_1(t)] = \zeta_0^{(1,0)}(t) + \zeta_1^{(1,0)}(t)$ , and  $\mathbb{E}[\Theta_1(t)] = \zeta_0^{(0,1)}(t) + \zeta_1^{(0,1)}(t)$ . We will revisit this example in Section IV-A.  $\blacksquare$

#### D. Dynamic Reliability Assessment

With increased penetration of renewable resources and uncertain loads, dynamic reliability/risk assessment studies that can be performed with minimum computational burden will become increasingly important to ensure the reliable operation of next-generation power systems. In this section, we explore how upper bounds on the probability that the power-system dynamic and algebraic states satisfy certain performance requirements can be obtained with a few of their lower-order moments. To simplify notation, denote the  $i$  dynamic/algebraic state of the power system at time  $t$  by  $z_i(t)$ , and the corresponding stochastic process by  $Z_i(t)$ . Suppose that performance requirements establish the maximum and minimum values that  $z_i$  can take at any time. In other words, the acceptable range for  $z_i(t)$  is denoted by  $\mathcal{R}_{z_i} := [z_i^{\min}, z_i^{\max}]$ , and we want to ensure that in spite

of active/reactive power-injection disturbances in the system,  $z_i(t) \in \mathcal{R}_{z_i} \forall t$ . Acknowledging the uncertainty in power injections, we establish the following probabilistic risk notion

$$\rho_{z_i}(t) := \Pr \{Z_i(t) \notin \mathcal{R}_{z_i}\} = 1 - \Pr \{z_i^{\min} \leq Z_i(t) \leq z_i^{\max}\}. \quad (40)$$

Said in words,  $\rho_{z_i}(t)$  denotes the probability that the  $i$  dynamic/algebraic state does not satisfy the performance requirements. One method to compute  $\rho_{z_i}(t)$  is through repeated Monte Carlo simulations. In each simulation, load changes occur at random instants (based on the transition rates of the SHS), and repeated simulations yield a histogram from which (40) can be computed. While straightforward in conception and implementation, this procedure is patently computationally expensive. Alternatively, we can obtain the moments of  $Z_i(t)$ , i.e.,  $\mathbb{E}[Z_i^m(t)]$ ,  $m \in \mathbb{N}^+$ , using SHS formalisms and upper-bound  $\rho_{z_i}(t)$  using moment inequalities. For example, consider the following one-sided Chebyshev inequality (see, e.g., [50]):

$$\rho_{z_i}(t) \leq 1 - \frac{4 \left( (\mathbb{E}[Z_i(t)] - z_i^{\min}) (z_i^{\max} - \mathbb{E}[Z_i(t)]) \right)}{(z_i^{\max} - z_i^{\min})^2} - \frac{4\sigma_{Z_i(t)}^2}{(z_i^{\max} - z_i^{\min})^2} =: \bar{\rho}_{z_i}(t), \quad (41)$$

where  $\sigma_{Z_i(t)}$  is the standard deviation of  $Z_i(t)$ , given by

$$\sigma_{Z_i(t)} := \left( \mathbb{E}[Z_i^2(t)] - (\mathbb{E}[Z_i(t)])^2 \right)^{1/2}. \quad (42)$$

Essentially, (41) provides a method to compute upper bounds to the probability that the power system states do not meet performance requirements (i.e., the probability that they are not within the acceptable range) simply with their first- and second-order moments.

We want to point out that (41) is just one type of moment inequality that can be used in conjunction with the moment ODEs to obtain probabilistic notions of risk of the type in (40). Also, note that (41) is a conservative result in the sense that the actual probability of violating a performance objective is always lower than that obtained with the moment inequality. Depending on the number of known moments, different moment inequalities might yield results that are more or less conservative than that obtained with (41). In particular, note that more knowledge about higher-order moments can give sharper estimates than (41) as well (see, e.g., [51, §21]). An interesting avenue for future work would be to quantify conventional power system reliability metrics such as loss of load probability (see, e.g., [52]) within the proposed SHS-based framework.

#### IV. CASE STUDIES

In this section, we analyze three case studies. The first one presents numerical results for the SMIB system described in Examples 1–3. The second case study develops an SHS model for the standard three-machine-nine-bus Western Electricity Coordination Council (WECC) power system [4]. The third case study, which involves the IEEE 50-machine test system and 145 buses, demonstrates the scalability of the proposed SHS-based approach to the analysis of large power systems.

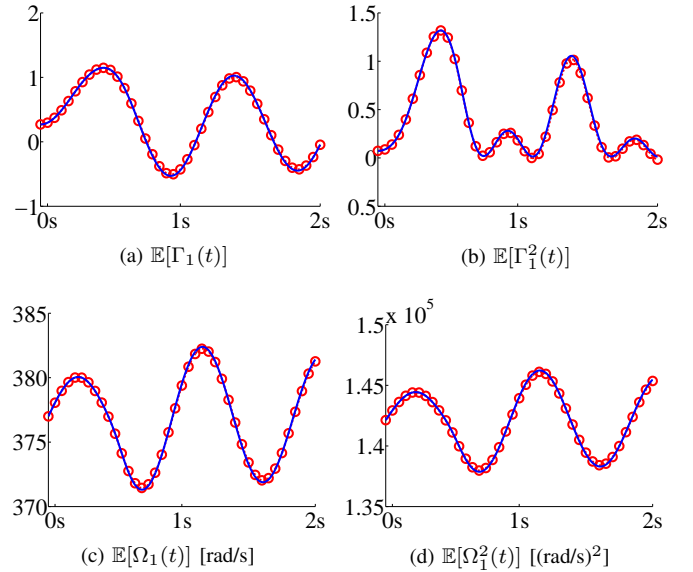


Figure 2. Moments of rotor angular position and speed. Results obtained from averaged Monte Carlo simulations (—) and SHS (●) are super imposed.

These case studies demonstrate that the proposed SHS framework can be utilized: i) for probabilistic dynamic performance/reliability assessment, and ii) to compute the steady-state statistics of relevant dynamic and algebraic states with far less computational burden compared to repeated Monte Carlo simulations. Unless stated otherwise, all quantities in the case studies are expressed in per unit (p.u.) with respect to an arbitrary base. As discussed in Remark 1, while the framework developed in Sections II and III can be extended to capture the impact of structural changes in a power system due to faults, in the case studies that follow, we just focus on uncertain variations in power injections that, e.g., could result from renewable-based generation resources.

##### A. Single-Machine Infinite-Bus Power System

Recall that in Example 3, we demonstrated how to obtain the ODEs that govern the moments of the dynamic and algebraic states for the two-mode SMIB SHS model. In this case study, we validate the accuracy of the proposed SHS framework by comparing the results with averaged Monte Carlo simulations, and utilize the approach outlined in Section III-D to investigate the dynamic reliability of this system.

The machine, network, and load parameter values for the simulations are adopted from [34], and listed in Appendix B-1. We will assume the duration of the period over which the load is not given by the nominal value is normally distributed with mean  $m_T = 0.5s$ , and standard deviation  $\sigma_T = \frac{10}{100} m_T$ . We will further assume that the active/reactive power injections in mode 1 are 10% of the nominal values. i.e.,  $P_1^1 = \frac{10}{100} P_1^0$  and  $Q_1^1 = \frac{10}{100} Q_1^0$ .

1) *Comparisons with Monte Carlo Simulations:* For the SMIB system described above, Figs. 2 (a)-(d) depict the first- and second-order moments of the dynamic states, i.e., the rotor angular position and velocity. Figures 3 (a)-(d) depict the first- and second-order moments of the algebraic states, i.e.,

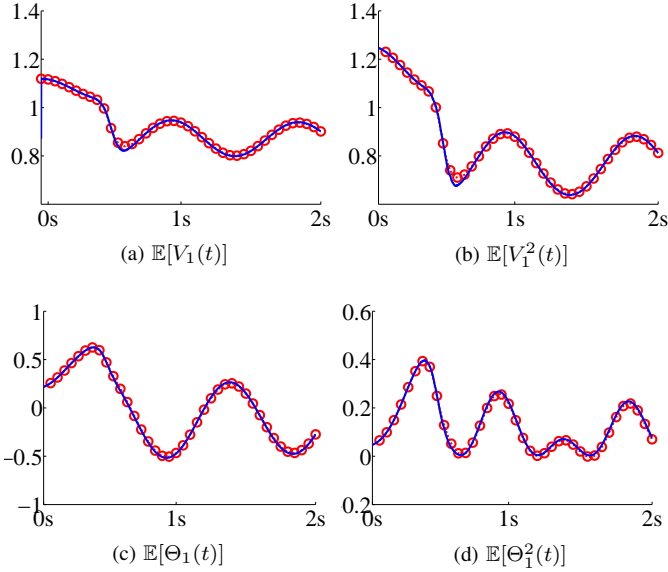


Figure 3. Moments of bus-voltage magnitude and angle. Results obtained from averaged Monte Carlo simulations (—) and SHS (●) are super imposed.

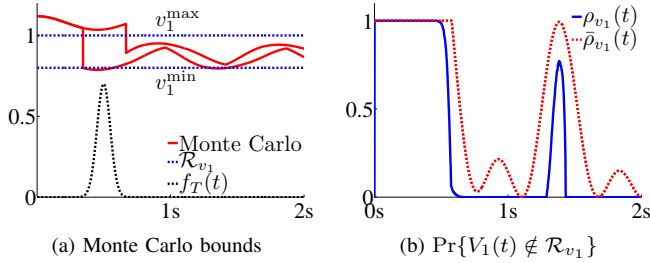


Figure 4. Dynamic performance/reliability assessment.

the bus 1 voltage magnitude and angle. The results obtained with the SHS framework are superimposed on those obtained by averaging the results of 1000 Monte Carlo simulations. Note that in Example 3, we demonstrated how to obtain the first-order moments of the dynamic and algebraic states, i.e.,  $\mathbb{E}[\Gamma_1(t)]$ ,  $\mathbb{E}[\Omega_1(t)]$ ,  $\mathbb{E}[V_1(t)]$ , and  $\mathbb{E}[\Theta_1(t)]$ . Following a similar procedure, and for the purpose of this case study, the second-order moments of the dynamic and algebraic states are obtained by substituting  $m = (m_1, m_2) = (2, 0)$  and  $m = (0, 2)$  in (31) and (34), respectively, and using the law of total expectation as described in (23). The SHS results match those obtained by averaging the results of repeated simulations perfectly. The computer execution time to obtain the first- and second-order moments with the SHS approach was 0.189 s, compared to 18.3 s for the repeated Monte Carlo simulations.

2) *Dynamic Reliability Assessment*: Suppose performance requirements dictate that the bus 1 voltage magnitude be constrained to the range  $\mathcal{R}_{v_1} = [v_1^{\min}, v_1^{\max}] = [0.8, 1]$ . Figure 4(a) depicts these bounds as well as the maximum and minimum values of the bus 1 voltage magnitude obtained from 1000 Monte Carlo simulations. A scaled version of the  $f_T(t)$ , is also shown for comparison. Figure 4 (b) shows: i)  $\rho_{v_1}(t)$ , the probability that the bus 1 voltage magnitude is not within

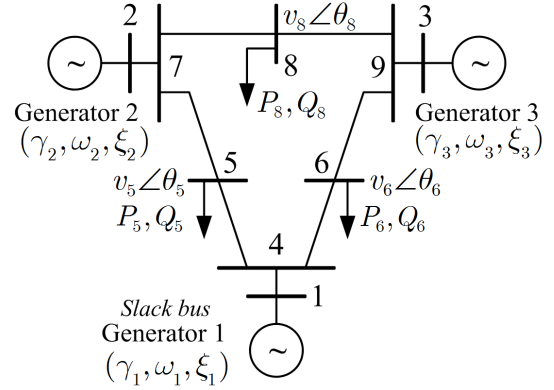


Figure 5. One-line diagram of the WECC three-machine nine-bus power system studied in Section IV-B.

the acceptable range computed numerically from the Monte Carlo simulations, and ii)  $\bar{\rho}_{v_1}(t)$ , an upper bound to  $\rho_{v_1}(t)$  computed by substituting the first- and second-order moments of  $V_1(t)$  in (41). The results indicate the time periods where there is a high probability of the bus 1 voltage magnitude not meeting the performance requirements. We want to stress that while the analytical result is obtained by the simulation of a few ODEs, the numerical results are obtained from 1000 Monte Carlo simulations. While the analytical results are conservative, as described in Section IV-A1, they are computationally inexpensive to obtain.

### B. Three-Machine Nine-Bus Power System

In this case study, we model stochastic variations in active/reactive power injections in a three-machine nine-bus power system within the SHS framework. Particularly, the active/reactive power injections are modeled as a Markov process; in SHS terminology, this means that the transition rates are constant. We utilize the SHS framework to compute the moments of the synchronous-generator dynamic states and the bus-voltage magnitudes and angles. As with the SMIB system examined earlier, we first compare the moments obtained from the SHS framework with those obtained by averaging the results of Monte Carlo simulations. Next, we examine the impact of the transition rates and the magnitude of the power injection in the non-nominal mode (i.e., the amount by which the power injections diverge away from the nominal values) on the steady-state moments of relevant dynamic and algebraic states.

1) *Electromechanical Model Description*: Consider the three-machine nine-bus system depicted in Fig. 5. We utilize a reduced-order model for the synchronous machines in the power system. The machine, network, and load parameter values for the simulations are adopted from [4], and listed in Appendix B-2. Particularly, the conventional nine-state synchronous machine model—that includes mechanical equations of motion, exciter, voltage regulator, turbine, governor, and models for the damper windings—is reduced to a three-state model that captures the governor dynamics and the mechanical equations of motion [53]. For the  $i^{\text{th}}$  synchronous machine, the system states of interest are the rotor angular position  $\gamma_i$ ,

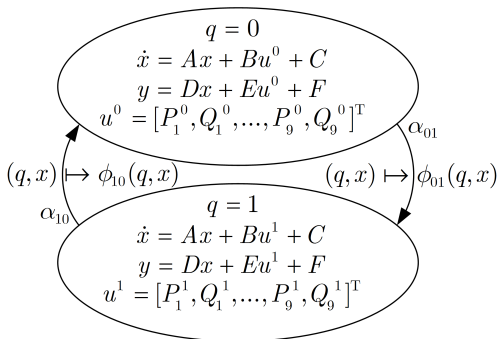


Figure 6. State-transition diagram for the SHS model of the WECC three-machine nine-bus power system studied in Section IV-B.

rotor angle velocity  $\omega_i$ , and the turbine power  $\xi_i$ . The evolution of these states is governed by

$$\begin{aligned} \dot{\gamma}_i &= \omega_i - \omega_s, \\ \dot{\omega}_i &= \frac{1}{M_i} \left( \xi_i - \frac{E_i V_i}{X_{M_i}} \sin(\gamma_i - \theta_i) - D_i (\omega_i - \omega_s) \right), \\ \dot{\xi}_i &= \frac{1}{T_i} \left( -(\xi_i - P_i^{\text{ref}}) - \frac{1}{R_{D_i} \omega_s} (\omega_i - \omega_s) \right), \end{aligned} \quad (43)$$

where  $\omega_s$  is the synchronous speed (377 rad/s),  $M_i$  is the machine inertia constant,  $X_{M_i}$  is the machine impedance,  $D_i$  is the damping coefficient,  $E_i$  is the machine internal voltage,  $T_i$  is the governor time constant,  $R_{D_i}$  is the slope of the machine speed-droop characteristic, and  $P_i^{\text{ref}}$  is a function of the unit base-point generation [53]. The states of the  $i$  generator are described by the vector  $x_i = [\gamma_i, \omega_i, \xi_i]^T$ , and the vector  $x = [x_1^T, x_2^T, x_3^T]^T$ ,  $x \in \mathbb{R}^{9 \times 1}$  captures all the dynamic states of the system. The power flow equations for the buses  $j = 1, \dots, 9$  are given by

$$\begin{aligned} \sum_{k=1}^9 V_k V_j (G_{kj} \cos(\theta_k - \theta_j) + B_{kj} \sin(\theta_k - \theta_j)) - P_j &= 0, \\ \sum_{k=1}^9 V_k V_j (G_{kj} \sin(\theta_k - \theta_j) - B_{kj} \cos(\theta_k - \theta_j)) - Q_j &= 0, \end{aligned} \quad (44)$$

where  $G_{kj}$  and  $B_{kj}$  are the conductance and susceptance, respectively, of the transmission line between bus  $k$  and  $j$ .

2) *Stochastic Active/Reactive Power-Injection Model*: We will assume that the active/reactive power injections in the buses are uncertain. Towards this end, consider a nominal mode where the active/reactive power injections at the buses are denoted by  $u^0 = [P_1^0, Q_1^0, \dots, P_9^0, Q_9^0]^T = [P_1^*, Q_1^*, \dots, P_9^*, Q_9^*]^T$ . Linearizing (43) and (44) about the equilibrium point corresponding to the nominal power injections, we get the system in (2). Now, consider a case where the active/reactive power injections are given by  $u^1 = [P_1^1, Q_1^1, \dots, P_9^1, Q_9^1]^T$ . As done in [39]–[41], we assume that the discrete process that governs the load is described by a Markov process. In particular, the transition rate that governs the  $0 \rightarrow 1$  transition is given by  $\lambda_{01}(q, t) = \delta_q(0)\alpha_{01}$ , and the rate that governs the  $1 \rightarrow 0$  transition is given by  $\lambda_{10}(q, t) = \delta_q(1)\alpha_{10}$ . The above model can be cast as an

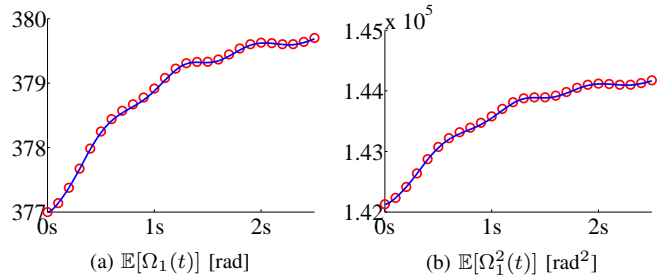


Figure 7. Moments of Generator 1 rotor angular speed. Results obtained from averaged Monte Carlo simulations (—) and SHS (●) are super imposed.

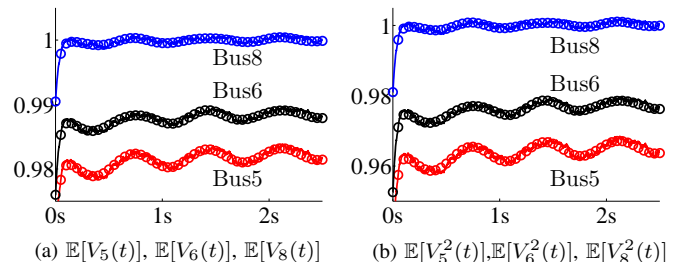


Figure 8. Moments of voltage magnitude at buses 5, 6, and 8. Results obtained from the SHS model (circles) are superimposed on those obtained by averaging the results of repeated Monte Carlo simulations (solid lines).

SHS with two modes: a nominal mode  $q = 0$  (with active/reactive power injections given by the nominal values  $P_j^0, Q_j^0, j = 1, \dots, 9$ ), and a mode  $q = 1$  (with the active/reactive power injections  $P_j^1, Q_j^1, j = 1, \dots, 9$ ). Finally, since  $\gamma_i, \omega_i$ , and  $\xi_i$  do not change instantaneously with transitions of the active/reactive power injections, the reset maps are given by  $\phi_{01}(q, x) = (1, x)$  and  $\phi_{10}(q, x) = (0, x)$ . The SHS described above is illustrated in Fig. 6.

3) *Moments of Dynamic and Algebraic States*: Suppose  $\alpha_{10} = 3/60 \text{ s}^{-1}$  and  $\alpha_{01} = 1.5/60 \text{ s}^{-1}$ . We will further assume that the active/reactive power injections in mode 1 are 50% of the nominal values, i.e.,  $P_i^1 = \frac{50}{100} P_i^0 = \frac{50}{100} P_i^*$ , and  $Q_i^1 = \frac{50}{100} Q_i^0 = \frac{50}{100} Q_i^*$ . For the system described above, Figs. 7(a)-(b) depict the first- and second-order moments of the Generator 1 rotor angular speed, and Figs. 8 (a)-(b) depict the first-and second-order moments of the voltage magnitude at buses 5, 6, and 8 (in this case study and the next, we focus on these buses without loss of generality because they have non-zero power injections [4]). In both cases, the results obtained from the SHS framework are superimposed on those obtained by averaging the results of 4000 Monte Carlo simulations.

### C. 145-Bus Case Study

In this section, we demonstrate the scalability of the proposed SHS-based framework to the analysis of large power systems. Particularly, we examine the IEEE 50-machine test system, which consists of 145 buses and 453 lines including 52 fixed tap transformers. A detailed description of its dynamic and static parameters can be found in [54]. To implement our analysis method, we use the small-signal stability analysis capability of the MATLAB-based Power Systems Toolbox (PST) [55]. Each of the 50 generator units are modeled by the mechanical equations of motion (2 states). Deviations in

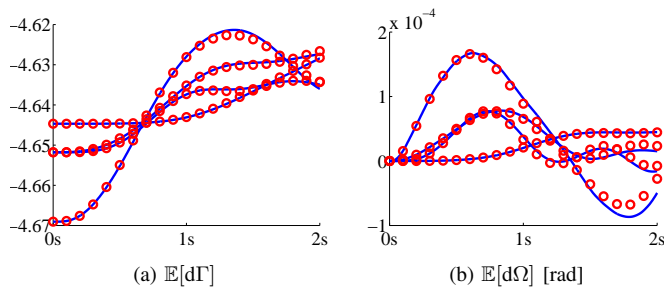


Figure 9. Expected values of rotor angle and frequency deviations for 145-bus test case. States of generators 1, 31, 45, and 91 are depicted.

generator rotor angles and speeds from the nominal steady-state values (denoted by  $d\Gamma$  and  $d\Omega$ , respectively) are adopted as system states. It is assumed that the real power injections in buses 74, 78, 81, 88, and 123 are uncertain and described by the Markov process in Fig. 6. We also ignore all reset maps for ease of analysis. Figures 9 (a) and 9 (b) depict the first-order moments of rotor speeds and angular velocity deviations for generators 1, 35, 45, and 91. Results obtained by averaging 200 Monte Carlo simulations are superimposed. The computer execution time to obtain the moments with the SHS approach was 0.07s, compared to 16.1s for the repeated Monte Carlo simulations.

## V. CONCLUSIONS AND FUTURE WORK

This work presented a framework to analyze small-signal active/reactive power-injections stochastic variations in power systems. The moments of the dynamic states of the power system (generator speeds and angles) are obtained by the solution of ODEs formulated using Dynkin's formula. The moments of the algebraic states can then be recovered straightforwardly from the moments of the dynamic states. We demonstrated several applications of the proposed framework including methods for dynamic reliability/risk assessment and steady-state analysis of relevant dynamic- and algebraic-state moments. As part of future work, we will investigate models where the transition rates could be a function of the dynamic and algebraic states. Additionally, we will develop a computational platform to scale the proposed framework to large power systems with more detailed generator dynamic models.

## APPENDIX

### A. Derivation of Linearized Power-System Model in (2)

Recall the standard power-system DAE model in (1). Denote the Jacobian of  $f(\cdot, \cdot)$  and  $g(\cdot, \cdot, \cdot)$  evaluated at  $(x^*, y^*, u^*)$  by

$$J_f|_{(x^*, y^*)} = \left[ \frac{\partial f}{\partial x} \Big|_{(x^*, y^*)}, \frac{\partial f}{\partial y} \Big|_{(x^*, y^*)} \right]^T =: [f_x, f_y]^T, \quad (45)$$

$$J_g|_{(x^*, y^*, u^*)} = \left[ \frac{\partial g}{\partial x} \Big|_{(x^*, y^*, u^*)}, \frac{\partial g}{\partial y} \Big|_{(x^*, y^*, u^*)}, \frac{\partial g}{\partial u} \Big|_{(x^*, y^*, u^*)} \right]^T =: [g_x, g_y, g_u]^T. \quad (46)$$

Linearizing  $f(\cdot, \cdot)$  about the equilibrium point, up to first order, we get

$$\begin{aligned} \dot{x} &\approx f(x^*, y^*) + f_x(x - x^*) + f_y(y - y^*) \\ &= f_x x + f_y y - f_x x^* - f_y y^*, \end{aligned} \quad (47)$$

where we have used the fact  $f(x^*, y^*) = 0$ . Similarly, linearizing  $g(\cdot, \cdot, \cdot)$  about the equilibrium point,

$$0 \approx g(x^*, y^*, u^*) + g_x(x - x^*) + g_y(y - y^*) + g_u(u - u^*).$$

Assuming that  $g_y = \partial g / \partial y|_{(x^*, y^*, u^*)}$  is invertible, and recognizing that  $g(x^*, y^*, u^*) = 0$ , we get

$$y \approx g_y^{-1}(-g_x(x - x^*) - g_u(u - u^*) + g_y y^*). \quad (48)$$

Finally, substituting for  $y$  from (48) in (47), we get the linear system  $\dot{x} = Ax + Bu + C$  in (2), with  $A$ ,  $B$ , and  $C$  given by

$$\begin{cases} A = f_x - f_y g_y^{-1} g_x, \\ B = -f_y g_y^{-1} g_u, \\ C = (g_y^{-1} g_x - f_x) x^* + g_y^{-1} g_u u^*. \end{cases} \quad (49)$$

Further, we can express  $y = Dx + Eu + F$ , with  $D$ ,  $E$ , and  $F$  given by

$$\begin{cases} D = -g_y^{-1} g_x, \\ E = -g_y^{-1} g_u, \\ F = g_y^{-1} g_x x^* + y^* + g_y^{-1} g_u u^*. \end{cases} \quad (50)$$

The proposed linearization approach hinges on the invertibility of the power-flow Jacobian. In extenuating cases such as voltage collapse [56]–[58], it is well known that the power-flow Jacobian may be singular. Constructing linearized models around such operating points is infeasible. Therefore, the proposed method is only applicable in cases where the power-flow solution exists, which implies that the power-flow Jacobian is invertible.

### B. Modeling Uncertain Power Injections with SDEs

To keep the size of the discrete state space manageable, the variability in the power injections can be captured by expressing  $u$  as a continuous stochastic process, the evolution of which is described by an SDE. To this end, consider the model in (9), and modify it by adding an additional driving term  $V(t)$  as follows:

$$\begin{aligned} dX(t) &= AX(t)dt + B(U(Q(t)) + V(t))dt + Cdt, \\ dV(t) &= G(Q(t))V(t)dt + H(Q(t))dW(t), \end{aligned} \quad (51)$$

where  $W(t)$  denotes a vector of independent standard Wiener processes, and  $G(Q(t))$  and  $H(Q(t))$  are matrices of appropriate dimensions. The dependence of the matrices  $G$  and  $H$  on  $Q(t)$  enables the statistics of  $V(t)$  to be different in each mode; thus providing increased modeling flexibility. The expressions in (51) above can be rewritten in matrix form as follows:

$$\begin{aligned} \begin{bmatrix} dX(t) \\ dV(t) \end{bmatrix} &= \begin{bmatrix} A & B \\ 0 & G(Q(t)) \end{bmatrix} \begin{bmatrix} X(t) \\ V(t) \end{bmatrix} dt \\ &+ \begin{bmatrix} B & I \\ 0 & 0 \end{bmatrix} \begin{bmatrix} U(Q(t)) \\ C \end{bmatrix} dt \\ &+ \begin{bmatrix} 0 \\ H(Q(t)) \end{bmatrix} dW(t), \end{aligned} \quad (52)$$

which can be compactly written as

$$d\tilde{X}(t) = (\tilde{A}(Q(t))\tilde{X}(t) + \tilde{B}(Q(t)))dt + \tilde{C}(Q(t))dW(t), \quad (53)$$

for appropriately defined  $\tilde{X}(t)$ ,  $\tilde{A}(Q(t))$ ,  $\tilde{B}(Q(t))$ , and  $\tilde{C}(Q(t))$ . The resulting extended generator is given by

$$\begin{aligned} (L\psi)(q, x) &= \frac{\partial}{\partial x} \psi(q, x) \cdot (\tilde{A}(q)\tilde{X}(t) + \tilde{B}(q)) \\ &+ \frac{1}{2} \sum_{\alpha, \beta} \left( (\tilde{C}(q)\tilde{C}^T(q))_{\alpha, \beta} \frac{\partial^2}{\partial x_\alpha \partial x_\beta} \psi(q, x) \right) \\ &+ \sum_{i, j \in \mathcal{Q}} \lambda_{ij}(q, x) (\psi(\phi_{ij}(q, x)) - \psi(q, x)), \quad (54) \end{aligned}$$

where the second term in the expression above captures the effect of the Wiener process [3], [47]. Going through the derivation similar to (24)-(31), we would get the following expression for the moment ODEs:

$$\begin{aligned} \dot{\mu}_i^{(m)}(t) &= \sum_{p=1}^n m_p \left( \sum_{r=1}^n a_{pr} \mu_i^{(m-e_p+e_r)}(t) + \mu_i^{(m-e_p)}(t) v_p^i \right) \\ &+ \frac{1}{2} \sum_{\alpha=1}^n \left( \tilde{c}_{\alpha\alpha} m_\alpha (m_\alpha - 1) \mu_i^{(m-2e_\alpha)}(t) \right. \\ &\quad \left. + \sum_{\beta \neq \alpha} \tilde{c}_{\alpha\beta} m_\alpha m_\beta \mu_i^{(m-e_\alpha-e_\beta)}(t) \right) \\ &+ \sum_{j \in \mathcal{Q}_i^-} \alpha_{ji}(t) \mu_j^{(m)}(t) - \sum_{k \in \mathcal{Q}_i^+} \alpha_{ik}(t) \mu_i^{(m)}(t), \quad (55) \end{aligned}$$

where  $\tilde{c}_{\alpha\beta}$  is the  $(\alpha, \beta)$  element of  $\tilde{C}\tilde{C}^T$ .

### C. Parameter Values for Case Studies

1) *Single-Machine Infinite Bus System*: The parameters for this example are adopted from [34]. The synchronous speed,  $\omega_s=377$  rad/s; the machine inertia constant,  $M = 7/\omega_s$ ; the machine damping coefficient,  $D = 2/\omega_s$ , the machine impedance,  $X_M = 0.45$ ; the impedance between bus 1 and 2,  $X_L = 0.5$ ; the machine internal voltage,  $E = 1.1$ ; and the turbine set-point  $P_M = 0.8$ . For the nominal active/reactive power injections, i.e., for  $P_1^0 = P_1^* = 1$ ,  $Q_1^0 = Q_1^* = 0.5$ , solving the power flow gives us the following nominal values of the dynamic and algebraic states:  $\gamma^* = 0.2701$ ,  $\omega^* = 377$  rad/s,  $v_1^* = 0.871$ ,  $\theta_1^* = -0.115$ .

2) *Three-Machine Nine-Bus System*: The parameters for this example are adopted from [4]. A few relevant parameters are provided next. The system base MVA is 100; the synchronous speed,  $\omega_s=377$  rad/s; the machine inertia constants,  $M_1 = 0.1254$ ,  $M_2 = 0.0340$ , and  $M_3 = 0.0160$ ; the machine damping coefficients,  $D_1 = 0.0125$ ,  $D_2 = 0.0068$ ,  $D_3 = 0.0048$ ; the machine impedances,  $X_{M_1} = 0.0608$ ,  $X_{M_2} = 0.1198$ ,  $X_{M_3} = 0.1813$ ; the machine internal voltages,  $E_1 = 1.0563$ ,  $E_2 = 1.0499$ ,  $E_3 = 1.0169$ ; and  $P_1^{\text{ref}} = 0.64$ ,  $P_2^{\text{ref}} = 1.63$ ,  $P_3^{\text{ref}} = 0.85$ .

### REFERENCES

- [1] A. D. Domínguez-García, "Reliability modeling of cyber-physical electric power systems: A system-theoretic framework," in *IEEE Power and Energy Society General Meeting*, in press, 2012.
- [2] B. Parsons *et al.*, "Grid impacts of wind power variability: Recent assessments from a variety of utilities in the United States," National Renewable Energy Laboratory, Tech. Report NREL/CP-500-39955, 2006.
- [3] J. P. Hespanha, "Modelling and analysis of stochastic hybrid systems," *IEEE Proceedings—Control Theory and Applications*, vol. 153, no. 5, pp. 520–535, September 2006.
- [4] P. Sauer and M. A. Pai, *Power System Dynamics and Stability*. Upper Saddle River, NJ: Prentice Hall, 1998.
- [5] P. Kundur, J. Paserba, V. Ajjarapu, G. Andersson, A. Bose, C. Canizares, N. Hatziaargyriou, D. Hill, A. Stankovic, C. Taylor, T. V. Cutsem, and V. Vittal, "Definition and classification of power system stability IEEE/CIGRE joint task force on stability terms and definitions," *IEEE Transactions on Power Systems*, vol. 19, no. 3, pp. 1387–1401, August 2004.
- [6] Y. C. Chen and A. D. Domínguez-García, "A method to study the effect of renewable resource variability on power system dynamics," *IEEE Transactions on Power Systems*, vol. 27, no. 4, pp. 1978–1989, November 2012.
- [7] J. Endrenyi, *Reliability Modeling in Electric Power Systems*. New York, NY: John Wiley and Sons, 1978.
- [8] O. Ardakanian, S. Keshav, and C. Rosenberg, "Markovian models for home electricity consumption," in *Proceedings of the 2nd ACM SIGCOMM workshop on Green networking*, 2011, pp. 31–36.
- [9] Y. Manichaikul and F. C. Schweppe, "Physically based industrial electric load," *IEEE Transactions on Power Apparatus and Systems*, vol. PAS-98, no. 4, pp. 1439–1445, July 1979.
- [10] S. Koch, J. L. Mathieu, and D. S. Callaway, "Modeling and control of aggregated heterogeneous thermostatically controlled loads for ancillary services," in *Power Systems Computation Conference*, August 2011.
- [11] F. F. C. Véliz, C. L. T. Borges, and A. M. Rei, "A comparison of load models for composite reliability evaluation by nonsequential Monte Carlo simulation," *IEEE Transactions on Power Systems*, vol. 25, no. 2, pp. 649–656, May 2010.
- [12] R. Malhamé and C. Y. Chong, "Electric load model synthesis by diffusion approximation of a high-order hybrid-state stochastic system," *IEEE Transactions on Automatic Control*, vol. 30, no. 9, pp. 854–860, September 1985.
- [13] —, "Stochastic hybrid state systems for electric load modeling," in *IEEE Conference on Decision and Control*, vol. 22, December 1983, pp. 1143–1149.
- [14] R. Malhamé, "A jump-driven Markovian electric load model," *Advances in Applied Probability*, vol. 22, no. 3, pp. 564–586, September 1990.
- [15] C. Y. Chong and A. S. Debs, "Statistical synthesis of power system functional load models," in *IEEE Conference on Decision and Control including the Symposium on Adaptive Processes*, vol. 18, December 1979, pp. 264–269.
- [16] G. Papaefthymiou and B. Klöckl, "MCMC for wind power simulation," *IEEE Transactions on Energy Conversion*, vol. 23, no. 1, pp. 234–240, March 2008.
- [17] A. P. Leite, C. L. T. Borges, and D. M. Falcão, "Probabilistic wind farms generation model for reliability studies applied to Brazilian sites," *IEEE Transactions on Power Systems*, vol. 21, no. 4, pp. 1493–1501, November 2006.
- [18] P. S. Perez, J. Driesen, and R. Belmans, "Characterization of the solar power impact in the grid," in *International Conference on Clean Electrical Power*, May 2007, pp. 366–371.
- [19] R. J. Aguiar, M. Collares-Pereira, and J. P. Conde, "Simple procedure for generating sequences of daily radiation values using a library of Markov transition matrices," *Solar Energy*, vol. 40, no. 3, pp. 269–279, 1988.
- [20] H. A. Pulgar-Painemal, "Wind farm model for power system stability analysis," Ph.D. dissertation, University of Illinois at Urbana-Champaign, Urbana, IL, 2010.
- [21] —, "Towards a wind farm reduced-order model," *Electric Power Systems Research*, vol. 81, no. 8, pp. 1688–1695, 2011.
- [22] D. L. King, W. E. Boyson, and J. A. Kratochvil, "Photovoltaic array performance model," Sandia National Laboratories, Tech. Rep., August 2004.
- [23] D. L. King, S. Gonzalez, G. M. Galbraith, and W. E. Boyson, "Performance model for grid-connected photovoltaic inverters," Sandia National Laboratories, Tech. Rep., September 2007.
- [24] I. A. Hiskens and M. A. Pai, "Trajectory sensitivity analysis of hybrid systems," *IEEE Transactions on Circuits and Systems I: Fundamental Theory and Applications*, vol. 47, no. 2, pp. 204–220, February 2000.
- [25] —, "Hybrid systems view of power system modelling," in *IEEE International Symposium on Circuits and Systems*, vol. 2, 2000, pp. 228–231.

- [26] I. A. Hiskens, "Power system modeling for inverse problems," *IEEE Transactions on Circuits and Systems I: Regular Papers*, vol. 51, no. 3, pp. 539–551, March 2004.
- [27] Y. Susuki, H. Ebina, and T. Hikihara, "Application of hybrid system theory to power system stability analysis," in *International Symposium on Nonlinear Theory and its Applications*, 2005, pp. 202–205.
- [28] G. K. Furlas, K. J. Kyriakopoulos, and C. D. Vournas, "Hybrid systems modeling for power systems," *IEEE Circuits and Systems Magazine*, vol. 4, no. 3, pp. 16–23, 2004.
- [29] F. F. Wu and Y.-K. Tsai, "Probabilistic dynamic security assessment of power systems-I: Basic model," *IEEE Transactions on Circuits and Systems*, vol. 30, no. 3, pp. 148–159, March 1983.
- [30] K. Loparo and G. Blankenship, "A probabilistic mechanism for small disturbance instabilities in electric power systems," *IEEE Transactions on Circuits and Systems*, vol. 32, no. 2, pp. 177–184, February 1985.
- [31] C. O. Nwankpa and S. M. Shahidehpour, "Stochastic model for power system planning studies," *IEEE Proceedings-C, Generation, Transmission and Distribution*, vol. 138, no. 4, pp. 307–320, July 1991.
- [32] C. O. Nwankpa, S. M. Shahidehpour, and Z. Schuss, "A stochastic approach to small disturbance stability analysis," *IEEE Transactions on Power Systems*, vol. 7, no. 4, pp. 1519–1528, November 1992.
- [33] H. Mohammed and C. O. Nwankpa, "Stochastic analysis and simulation of grid-connected wind energy conversion system," *IEEE Transactions on Energy Conversion*, vol. 15, no. 1, pp. 85–90, March 2000.
- [34] K. Wang and M. L. Crow, "Numerical simulation of stochastic differential algebraic equations for power system transient stability with random loads," in *IEEE Power and Energy Society General Meeting*, July 2011, pp. 1–8.
- [35] T. Odun-Ayo and M. L. Crow, "Structure-preserved power system transient stability using stochastic energy functions," *IEEE Transactions on Power Systems*, vol. 27, no. 3, pp. 1450–1458, August 2012.
- [36] Z. Y. Dong, J. H. Zhao, and D. J. Hill, "Numerical simulation for stochastic transient stability assessment," *IEEE Transactions on Power Systems*, vol. 27, no. 4, pp. 1741–1749, November 2012.
- [37] F. F. Wu and S. Kumagai, "Steady-state security regions of power systems," *IEEE Transactions on Circuits and Systems*, vol. 29, no. 11, pp. 703–711, November 1982.
- [38] R. Kaye and F. F. Wu, "Dynamic security regions of power systems," *IEEE Transactions on Circuits and Systems*, vol. 29, no. 9, pp. 612–623, September 1982.
- [39] V. A. Ugrinovskii and H. R. Pota, "Decentralized control of power systems via robust control of uncertain Markov jump parameter systems," in *IEEE Conference on Decision and Control*, vol. 4, December 2004, pp. 3503–3508.
- [40] —, "Decentralized control of power systems via robust control of uncertain Markov jump parameter systems," *International Journal of Control*, vol. 78, no. 9, pp. 662–677, June 2005.
- [41] L. Li, V. A. Ugrinovskii, and R. Orsi, "Decentralized robust control of uncertain Markov jump parameter systems via output feedback," *Automatica*, vol. 43, no. 11, pp. 1932–1944, November 2007.
- [42] X. Ge, S. Parise, and P. Smyth, "Clustering Markov states into equivalence classes using SVD and heuristic search algorithms," in *International Workshop on Artificial Intelligence and Statistics*, 2003.
- [43] K. Deng, P. G. Mehta, and S. P. Meyn, "A simulation-based method for aggregating Markov chains," in *IEEE Conference on Decision and Control*, December 2009, pp. 4710–4716.
- [44] G. Kotsalis and M. Dahleh, "Model reduction of irreducible Markov chains," in *IEEE Conference on Decision and Control*, vol. 6, December 2003, pp. 5727–5728.
- [45] G. Kotsalis, A. Megretski, and M. A. Dahleh, "Model reduction of discrete-time Markov jump linear systems," in *American Control Conference*, June 2006, pp. 454–459.
- [46] J. P. Hespanha, "A Model for Stochastic Hybrid Systems with Application to Communication Networks," *Nonlinear Analysis, Special Issue on Hybrid Systems*, vol. 62, no. 8, pp. 1353–1383, September 2005.
- [47] S. V. Dhople, L. DeVille, and A. D. Domínguez-García, "A Stochastic Hybrid Systems framework for performability assessment," in review, 2012.
- [48] M. H. A. Davis, *Markov Models and Optimization*. Boundary Row, London: Chapman and Hall, 1993.
- [49] J. R. Norris, *Markov Chains*. New York, NY: Cambridge University Press, 1997.
- [50] K. Steliga and D. Szynal, "On Markov-type inequalities," *International Journal of Pure and Applied Mathematics*, vol. 58, no. 2, pp. 137–152, 2010.
- [51] P. Billingsley, *Probability and measure*, 3rd ed., ser. Wiley Series in Probability and Mathematical Statistics. New York: John Wiley & Sons Inc., 1995, a Wiley-Interscience Publication.
- [52] R. Billinton and R. N. Allan, *Reliability Evaluation of Power Systems*. Springer, 1996.
- [53] A. D. Domínguez-García, "Models for Impact Assessment of Wind-Based Power Generation on Frequency Control," in *Control and Optimization Methods for Electric Smart Grids*, (ed.) A. Chakraborty, and M. Ilić. Berlin: Springer-Verlag, 2012.
- [54] University of Washington. (2012, Oct.) Power system test case archive. [Online]. Available: <http://www.ee.washington.edu/research/pstca/>
- [55] Power system toolbox. [Online]. Available: <http://www.eps.ee.kth.se/personal/vanfretti/pst>
- [56] Y. Zhang, W. Huang, Z. Liu, J. Yang, X. Cai, and J. Zhang, "Research on the relationship of the singular point for load flow jacobian matrix and the critical point of voltage collapse," in *Power Engineering Society General Meeting, 2005. IEEE*, June 2005, pp. 2939–2943.
- [57] Y. Wang, L. da Silva, and X. Wilsun, "Investigation of the relationship between ill-conditioned power flow and voltage collapse," *IEEE Power Engineering Review*, vol. 20, no. 7, pp. 43–45, July 2000.
- [58] P. W. Sauer and M. A. Pai, "Power system steady-state stability and the load-flow Jacobian," *IEEE Transactions on Power Systems*, vol. 5, no. 4, pp. 1374–1383, November 1990.

**Sairaj Dhople (S'09, M'13)** received the B.S., M.S., and Ph.D. degrees in electrical engineering, in 2007, 2009, and 2012, respectively, from the University of Illinois, Urbana-Champaign. He is currently an Assistant Professor in the Department of Electrical and Computer Engineering at the University of Minnesota (Minneapolis), where he is affiliated with the Power and Energy Systems research group. His research interests include modeling, analysis, and control of power electronics and power systems with a focus on renewable integration.

**Yu Christine Chen (S'10)** received the B.A.Sc. degree in Engineering Science (major in Electrical Engineering) from the University of Toronto in Canada in 2009 and the M.S. degree in Electrical Engineering from the University of Illinois at Urbana-Champaign in 2011. She is currently pursuing a Ph.D. degree in Electrical Engineering at the University of Illinois at Urbana-Champaign. Her research interests include power system dynamics and monitoring, and renewable resource integration.

**Lee DeVille** received a B.S. in mathematics and computer science from Tulane University in 1996 and a M.A. and Ph.D. degree in mathematics from Boston University, Boston, MA, in 2001. He is an Assistant Professor in the Mathematics Department at the University of Illinois at Urbana-Champaign, where he is affiliated with the Differential Equations and Probability areas. His research interests include stochastic processes and their applications to science and engineering.

**Alejandro D. Domínguez-García (S'02–M'07)** is an Assistant Professor in the Department of Electrical and Computer Engineering of the University of Illinois at Urbana-Champaign, where he is affiliated with the Power and Energy Systems area. His research interests are in the areas of system reliability theory and control, and their application to electric power systems, power electronics, and embedded electronic systems for safety-critical/fault-tolerant aircraft, aerospace, and automotive applications. He received the Ph.D. degree in Electrical Engineering and Computer Science from the Massachusetts Institute of Technology, Cambridge, MA, in 2007 and the degree of Electrical Engineer from the University of Oviedo (Spain) in 2001. After finishing his Ph.D., he spent some time as a post-doctoral research associate at the Laboratory for Electromagnetic and Electronic Systems of the Massachusetts Institute of Technology. Dr. Domínguez-García received the NSF CAREER Award in 2010, and the Young Engineer Award from the IEEE Power and Energy Society in 2012. He is also a Grainger Associate since 2011. He currently serves as an Associate Editor for the IEEE Transactions on Power Systems and the IEEE Power Engineering Letters.